Molecular Beam Measurement of the Hyperfine Structure and Zeeman Effect of $^{85}Rb^{19}F$

Craig D. Hollowell * and Florentin Lange

Physikalisches Institut der Universität Bonn

(Z. Naturforsch. **29 a**, 1548–1552 [1974]; received August 29, 1974)

Hyperfine structure and Zeeman effect of the $^{85}Rb^{19}F$ molecule have been measured with a molecular beam apparatus using electric four poles as deflecting fields and homogeneous superimposed electric and magnetic fields in the transition region. Electric dipole transitions were induced between the hyperfine structure levels of the first rotational state $J=1$ and the two lowest vibrational states $v=0$ and $v=1$ for the strong field case. The following quantities were determined and are compared with results from weak field measurements: the magnetic rotational dipole moment μ_J, the nuclear spin-rotational interactions c_1 and c_2 ($1 \triangleq$ Rb, $2 \triangleq$ F), the scalar and tensor part of the nuclear dipole-dipole interaction d_S and d_T, the quadrupole coupling constant eqQ of the Rb nucleus, the anisotropy of the magnetic susceptibility $\xi_\perp - \xi_\parallel$, the anisotropy of the magnetic shielding of the external magnetic field at the position of both nuclei $(\sigma_\perp - \sigma_\parallel)_1$ and $(\sigma_\perp - \sigma_\parallel)_2$, the magnetic moment of the Rb nucleus multiplied by the scalar part of the magnetic shielding tensor $\mu_1 (1-\sigma)_1$.

1. Introduction

In a preceding work [1] the hyperfine structure, Stark effect and Zeeman effect of the diatomic polar molecule ^{85}RbF had been measured in the $J=1$ rotational state with a molecular beam apparatus having combined homogeneous electric and magnetic fields in the transition region. Except for the determination of the electric dipole moment all these measurements were done in the weak field case, i. e. with partial coupling of the angular momenta of the molecule (nuclear spins, rotational angular momentum). The interaction energy of the electric quadrupole moment of the rubidium nucleus with the molecular electric field gradient ($70\ \mathrm{MHz}\cdot h$) is large compared to that of other alkali fluorides [2–6]. The weak field case for which the matrix elements of the quadrupole interaction diagonal in J are also fully diagonal in all other quantum numbers is better suited to the measurement of the hyperfine structure constants.

The strong field case which is characterized by the decoupling of the angular momenta I_1, I_2 and J is only realized at Stark effect energies comparable or larger than the quadrupole interaction. Adjusting the separation of the electrodes (5 mm), which produce the Stark field, to half an optical wavelength over the 8 cm long radiofrequency zone results in a relative homogeneity of 5×10^{-5}. This corresponds to a linewidth of 7 kHz at a (quadratic) Stark effect energy of $70\ \mathrm{MHz}\cdot h$. That is just sufficient to resolve lines which are separated by smaller effects like the nuclear spin – rotational interaction or the anisotropy of the diamagnetic shielding. At Stark effect energies as low as $45\ \mathrm{MHz}\cdot h$ all transitions were observed which are allowed in the strong field case. The observved line width was then 5 to 6 kHz and comparable with the natural line width of about 4 kHz resulting from the time of flight of the molecules through the transition region. The present measurements also allow a check to be made of the interaction constants with an external magnetic field, which were originally measured in the weak field case [1]. The precision of the measurements is in both cases comparable.

The molecular beam apparatus used for these studies is described in full detail elsewhere [7]. Velocity selected molecules in the rotational state $(J, m_J) = (1,0)$ were focussed on a hot tungsten-wire surface ionizer. The intensity of the focussed beam was 10 times bigger than the background which resulted mainly from the scattered beam. Hyperfine transitions $\Delta m_J = \pm 1$ were electrically induced in the transition region consisting of a homogeneous electric field with superimposed magnetic field. The resulting diminution of the beam intensity at the detector was about 2% and the resonance transitions could be measured with a

Reprints requests to Dr. F. Lange, Johannes Gutenberg-Universität, *D-6500 Mainz*, Jakob-Welder-Weg 11, West Germany.

* Present address: Lawrence Berkeley Lab. University of California, Berkeley, California.

signal – to – noise ratio of 8 : 1. By repeating the measurement of the spectrum 10 times the line centers could be determined to within 100 Hz. The magnetic field seen by the molecules could be determined to some 10^{-4}, the main limiting factor being the uncertainty in the position of the proton resonance probe. The highest magnetic field used was 7000 Gauss.

2. Hamiltonian Operator

The Hamiltonian operator of a diatomic polar molecule in a $^1\Sigma$-electronic ground state with $\boldsymbol{J}$ being the rotational angular momentum and $\boldsymbol{I}_1$ and $\boldsymbol{I}_2$ the two nuclear spins has the following form in an external electric field $\boldsymbol{E}$ and a magnetic field $\boldsymbol{H}$:

$$\begin{aligned}\mathcal{H} = {} & B\,\boldsymbol{J}^2 - (\mu_{el}\cdot\boldsymbol{E}) - \frac{\mu_1}{I_1}\boldsymbol{I}_1\cdot[1-\sigma_1(J)]\cdot\boldsymbol{H} \\ & - \frac{\mu_2}{I_2}\boldsymbol{I}_2\cdot[1-\sigma_2(J)]\cdot\boldsymbol{H} - \frac{\mu_J}{J}(\boldsymbol{J}\cdot\boldsymbol{H}) \\ & - \tfrac{1}{2}[\boldsymbol{H}\cdot\boldsymbol{\xi}(J)\cdot\boldsymbol{H}] + c_1(\boldsymbol{I}_1\cdot\boldsymbol{J}) + c_2(\boldsymbol{I}_2\cdot\boldsymbol{J}) \qquad (1) \\ & + [\boldsymbol{I}_1\cdot\boldsymbol{d}(J)\boldsymbol{I}_2] - \frac{1}{4I_1(2I_1-1)}[\boldsymbol{I}_1\cdot e\,\boldsymbol{q}\,\boldsymbol{Q}(J)\cdot\boldsymbol{I}_1]\,.\end{aligned}$$

The index 1 refers to the rubidium nucleus, and index 2 to the fluoride nucleus. The terms, in order, correspond to the following energy contributions: rotational energy, Stark effect of the molecule's permanent electric dipole moment with the externally applied electric field $\boldsymbol{E}$, Zeeman effect of the nuclei 1 and 2 in the external field $\boldsymbol{H}$ which is screened by the electron cloud, Zeeman effect of the rotation, interaction of the magnetic susceptibility, the corresponding nuclear dipole – rotation interactions, the magnetic spin – spin interaction and finally the interaction of the Rb nuclear electric quadrupole moment with the molecular electric field gradient. Except for the contribution $-\frac{1}{2}(\boldsymbol{E}\cdot\boldsymbol{\alpha}\cdot\boldsymbol{E})$ of the electric polarizability which can be neglected at the applied electric field strengths the Hamiltonian includes all bilinear interactions of the form $\boldsymbol{A}\,\boldsymbol{\tau}\,\boldsymbol{B}$ where $\boldsymbol{A}$ and $\boldsymbol{B}$ stand for one of the five available vectors $\boldsymbol{E}$, $\boldsymbol{H}$, $\boldsymbol{J}$, $\boldsymbol{I}_1$, $\boldsymbol{I}_2$ and $\boldsymbol{\tau}$ is a tensor of second rank. The scalar and directionally dependent components of the different tensors of the phenomenological Hamiltonian (1) can be expressed by the properties of the electrons and nuclei. These relations are quoted for example in the report [8]. They allow the calculation of the quadrupole moment of the electronic charge distribution, the decomposition of the rotational magnetic moment in the nuclear and electronic contributions and the separation of the tensor part of the screening in para- and diamagnetic contributions. This has been discussed previously for the case of ^{85}RbF[1]. Our results for the strong field case confirm the weak field measurements, we therefore refer to the discussion contained within this report.

3. Energy Matrix and Selection Rules

To evaluate the measured radio frequency spectra, the energy matrix of the Hamiltonian (1) was constructed in the decoupled representation $|J, m_J; I_1; m_1; I_2, m_2\rangle$. For the case $J=1$, $I_1=5/2$, $I_2=1/2$ this matrix is given in the report [9]. The Stark effect has only off-diagonal elements between J and $J\pm1$. Due to the size of the quadrupole interaction it is not sufficient to use only the energy matrix for $J=1$ together with the Stark effect perturbation up to second order. The reason is that the perturbation calculation in third order, which also takes into account matrix elements of $e\,q\,Q$ off-diagonal in J, gives, for the case of RbF, contributions up to 100 kHz. The energy matrix therefore had to be extended up to $J=3$. All matrix elements of the Hamiltonian diagonal in J were included and also those elements of $e\,q\,Q$ and the Stark effect which were off-diagonal in J. The contributions of all other interactions which are not diagonal in J are below 1 Hz and can be neglected. The energy matrix then consists of (192×192) elements. The computer did not have enough core space to diagonalize a matrix of this size. If one neglects transverse components of $\boldsymbol{H}$ ($\boldsymbol{E}_{\text{eff}}$, the effective electric field seen by the molecules is the axis of quantization) the energy matrix can then be subdivided into sections of constant $M=m_J+m_1+m_2$. These submatrices are smaller (50×50) and could be diagonalized by the computer. Figure 1 shows the $M=0$ submatrix and indicates which matrix elements of the Hamiltonian have been taken into account.

In passing through the magnetic field $\boldsymbol{H}$, the molecules see an additional electric field

$$\boldsymbol{E} = (\boldsymbol{v}/c)\times\boldsymbol{H}\,.$$

If the applied fields $\boldsymbol{E}$ and $\boldsymbol{H}$ are parallel in the laboratory system then the effective fields seen by the molecules differ by an angle ($\leqq 1^\circ$ for our

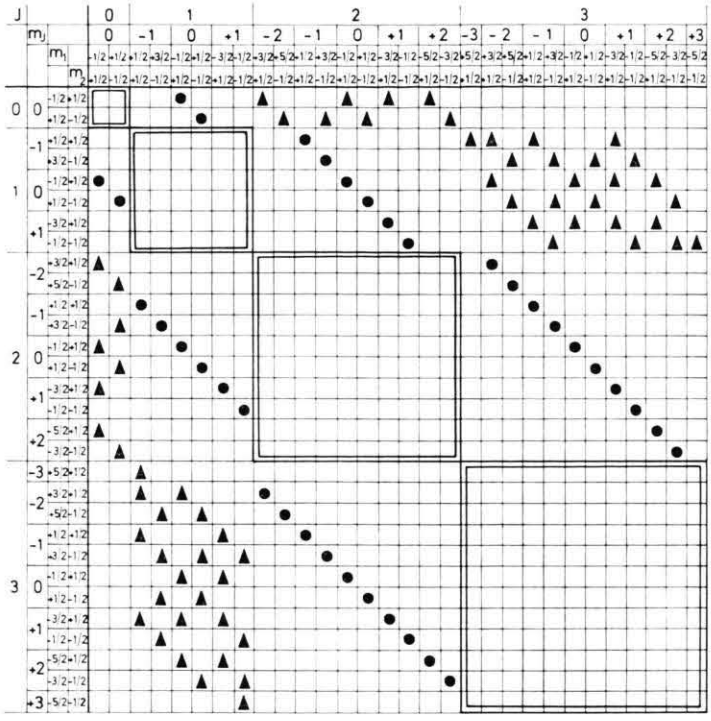

SUBMATRIX M = 0
$(M = m_J + m_1 + m_2)$

includes all in J diagonal matrix elements of the Hamiltonian.

- $\mu_z \cdot E_z$ (Stark-effect)
- ▲ $eq_1 Q_1$ (quadrupole interaction)

The diagonalization includes all in J diagonal matrix elements and in addition those matrix elements of $eq_1 Q_1$ and $\mu_z \cdot E_z$ which are off-diagonal in J. The axis of quantization is the direction of the effective electric field.

Fig. 1

Fig. 1. — — — — —

measuring condition). This gives rise to matrix elements which are not diagonal in M. These were taken into account by diagonalizing the whole $J = 1$ matrix.

In the case of radio frequency radiation perpendicular to the electric field the following selection rules apply

$$\Delta J = 0; \quad \Delta m_J = \pm 1; \quad \Delta m_1 = 0, \pm 2; \quad \Delta m_2 = 0 .$$

Transitions with $\Delta m_1 = \pm 2$ will take place since the quadrupole interaction has off-diagonal elements

$$\langle J, m_J; m_1, m_2 \,|\, e\,q\,Q \,|\, J, m_J \pm 2, m_1 \mp 2, m_2 \rangle$$

which are between energy levels degenerate with respect to the Stark effect and therefore couple these terms. These states differ by ± 2 in m_J, therefore two defocussed states are coupled and additional transitions are observed. The whole spectrum consists accordingly of 24 transitions with $\Delta m_1 = 0$ and a further 16 "coupled" transitions with $\Delta m_1 = \pm 2$. All these spectral lines were observed. Due to $\Delta m_1 = \pm 2$, the "coupled" transitions change the projection of I_1; these lines therefore allow the determination of the scalar part of the nuclear spin-spin interaction d_s and also the scalar part $\mu_1 (1 - \sigma_S)_1$ of the nuclear Zeeman effect.

4. Results and Discussion

The ^{85}RbF spectrum was measured for the vibrational ground state $v = 0$ and the first excited state $v = 1$ at 7 combinations of the electric and magnetic fields. For any combination of the two applied fields the spectrum was measured in 5 to 6 runs by scanning each spectral line back and forth. All those lines were measured for which the the splitting into two lines by c_2, d_T and $\mu_2 (1 - \sigma_S)_2$ was sufficiently large that they were well separated. The individual line width was 5 – 6 kHz. In addition, all those lines were measured for which this splitting was so small that the width (FWHM) of the resulting line did not exceed 5 to 6 kHz. In the analysis this was taken into account by taking the mean of the two corresponding linear equations. The analysis consisted essentially of the following procedure: the energy matrix was diagonalized with an initial set of constants; this allowed the evaluation of corrections to be applied to the measured frequencies before solving an over-determined system of linear equations giving a new set of constants. This iterating procedure was previously[6] described in greater detail.

For the evaluation of the molecular constants the following data were used:

$Y_{01} = 6315.548$ MHz $\quad \mu_F = 2.6287\ \mu_N$

$Y_{11} = -45.652$ MHz $\quad \mu_{Rb} = 1.348\ \mu_N$

$Y_{21} = 0.099$ MHz $\quad \mu_{el}(v=0) = 8.5464$ Deb

$\mu_{el}(v=1) = 8.6127$ Deb.

The measured molecular constants are summarized in Table I. The errors given in brackets for our results are three standard deviations, in units of the last decimal. For comparison we list the "best set" of values chosen from different measurements [10] which were all done for the weak field case. All Zeeman effect data were taken from the previous publication [1]. The results agree within the given errors. One can see that c_1 could be more precisely determined from the weak field case. The reason is that in this representation the matrix elements of c_1, the interaction between the magnetic moment of the Rb nucleus carrying the quadrupole moment and the magnetic field which arises from the molecule's rotational angular momentum are fully diagonal. One would have expected on the other hand that the interactions with the applied magnetic field could be determined more accurately for the strong field case for which the Zeeman effects of the nuclei and the rotation are fully diagonal in $J = 1$ for all quantum numbers. In addition the applied magnetic fields were almost a factor of two higher than for the weak field case measurements. The reason for not reaching a higher accuracy must be sought in the rather large off-diagonal elements of eqQ which also effect the accuracy of the data analysis. This is supported by the difference in accuracy of $(\sigma_\perp - \sigma_\parallel)_1$ and $(\sigma_\perp - \sigma_\parallel)_2$ for the strong field case. Comparing the combinations of linear equations that determine $(\sigma_\perp - \sigma_\parallel)_2$ with those for $(\sigma_\perp - \sigma_\parallel)_1$ one can see that in the first case the contributions from perturbation almost cancel, leading to a good accuracy in $(\sigma_\perp - \sigma_\parallel)_2$, while for the latter this is not so and the accuracy of $(\sigma_\perp - \sigma_\parallel)_1$ is rather poor.

For the weak field case the tensor part of the magnetic susceptibility can be determined from the measured spectrum at a fixed combination of electric and magnetic fields. This is not possible for the strong field case where $(\xi_\perp - \xi_\parallel)$ shifts all spectral lines by the same amount. This constant can therefore be determined from the center of mass shift of the spectrum at different magnetic fields keeping all other parameters fixed. The agreement of our measurement of $(\xi_\perp - \xi_\parallel)$ with the value from the weak field case is satisfactory considering the generally rather poor reproducibility in this measurements for other molecules.

Table I. Results (^{85}RbF; $J=1$).

	our results		"best values" [10]	
	$v=0$	$v=1$	$v=0$	$v=1$
$(eqQ)_1/h$ [kHz]	−70341.5 (22)	−69550.9 (84)	−70340.5 (4)	−69555 (2)
c_1/h [kHz]	0.465 (84)	1.4 (20)	0.525 (10)	0.52 (5)
c_2/h [kHz]	10.37 (47)	10.11 (52)	10.615 (60)	10.483 (100)
ds/h [kHz]	0.29 (21)	—	0.15 (5)	0.06 (12)
d_T/h [kHz]	0.76 (20)	0.84 (21)	0.93 (10)	0.77 (10)
μ_J/J [$10^{-6}\ \mu_B$]	29.73 (5)	29.63 (6)	−29.79 (2)	−29.71 (2)
$(\sigma_\perp - \sigma_\parallel)_1 \cdot 10^4$	−0.3 (30)	−0.3 (36)	−3.8 (21)	—
$(\sigma_\perp - \sigma_\parallel)_2 \cdot 10^4$	−3.12 (25)	−2.96 (30)	−2.6 (3)	—
$\mu_1(1-\sigma_s)_1$ [μ_N]	1.3483 (4)	—	1.3474 (5)	—
$(\xi_\perp - \xi_\parallel)$ [10^{-30} erg/G^2]	8 (4)	—	12 (6)	—

Acknowledgements

We would like to thank Professor W. Paul for advise and support and Professor G. Gräff for many stimulating discussions and his active help. We thank the Institut für Instrumentelle Mathematik for the opportunity of using the IBM 7090 computer. We also want to thank the Deutschen Forschungsgemeinschaft for supporting this experiment.

[1] G. Gräff, R. Schönwasser, and M. Tonutti, Z. Phys. **199**, 157 [1967].
[2] G. Gräff and Ö. Runolfsson, Z. Phys. **176**, 90 [1967].
[3] R. v. Boeckh, G. Gräff, and R. Ley, Z. Phys. **179**, 285 [1964].
[4] G. Gräff and G. Werth, Z. Phys. **183**, 223 [1965].
[5] G. Gräff and Ö. Runolfsson, Z. Phys. **187**, 140 [1965].
[6] J. Heitbaum and R. Schönwasser, Z. Naturforsch. **27 a**, 92 [1972].
[7] W. Drechsler and G. Gräff, Z. Phys. **163**, 165 [1961].
[8] R. Ley and W. Schauer, Z. Naturforsch. **27 a**, 78 [1972].
[9] F. Lange, Diplomarbeit, Bonn 1968.
[10] Landolt-Börnstein, Band 6, Molekülkonstanten, 1974.